The homeorhesis-based modelling and fast numerical analysis for oncogenic hyperplasia under radiotherapy

K. Psiuk-Maksymowicz*, E. Mamontov

Department of Physics, Göteborg University, Kemivägen 9, 412 96 Göteborg, Sweden

Abstract

A few previous works of the authors derived and discussed the space-time mathematical description, the PhasTraM model, for oncogenic hyperplasia regarded as a genotoxically activated homeorhetic dysfunction. The model is based on the fluid-to-solid-and-back transitions and nonlinear reaction-diffusion equation relevant to a series of the key biomedical facts and distinguishing features of living systems. The first computer-simulation results have also been reported. The present work generalizes the PhasTraM model for the effect of radiation therapies (RTs), both external and internal. The resulting model also includes the autocrine mechanism promoting oncogenic hyperplasia and the suppression of this process by certain drugs. The autocrine signalling is implemented by the transforming-growth-factor-α (TGF-α) molecules released by the cells and bound to the epidermal-growth-factor receptors (EGFRs) at the cell surface. The suppression can be carried out by a drug deactivating the mentioned molecules. The work also presents and discusses examples of the computer-simulation results for four different settings of the applied RT. A few directions for future research as well as prospective applications of the model and developed software are also discussed.

Keywords: Reaction-diffusion equation; Cauchy problem; Tumour; Oncogenic hyperplasia; Homeorhesis

1 Introduction

The ability of a living system to maintain a static equilibrium independently (in sufficiently large time intervals) of exogenous (external, coming from outside a system) signals bears name *homeostasis* [1]. An example of homeostasis is the ability of the body to maintain an internal temperature at a constant level, no matter what is the external temperature (within a certain range). *Homeorhesis* [2] is the time-dependent generalization of homeostasis. Homeorhesis concerns the dynamic rather than static equilibrium of the system, in which continuous changes of the steady state occurs.

A tumour is an abnormal new mass of tissue that results from uncontrolled division of the cells. Tumours perform no useful body function. They may be either benign (not cancerous) or malignant (cancerous). Oncogeny, i.e. formation of a tumour, progresses in a sequence of steps: hyperplasia, dysplasia, growth in situ, angiogenesis, and invasion. As it is well known in biomedicine, *oncogenic* hyperplasia is the first and therefore inevitable stage in development of any (solid) tumour. Oncogenic hyperplasia is also implicated in many other proliferative diseases: vascular; gastrointestinal; endocrine; proliferative dermatoses (infantile eczema and lichenification); megakaryocytic or platelet hyperplasia; hyperplasia of cardiac muscle; hyperplastic lesions of the larynx; ductal, prostatic, intimal, endometrial, and lymphoid hyperplasias; and others. Oncogenic hyperplasia is a process that is continuous in space and time where quantitative changes in the cell-population characteristics result in qualitative differences. As it is well known (e.g., [3, 4, 5]), oncogenic hyperplasia is a genotoxically activated homeorhetic dysfunction.

*Corresponding author. Tel.: +46 31 772 2097.
E-mail addresses: krzysztof.psiuk@physics.gu.se (K. Psiuk-Maksymowicz), yem@physics.gu.se (E. Mamontov).

The *minimal* mathematical model that takes into account the listed features was developed in [6] (see also [7, 8]). The purpose of the present work is three-fold:

- incorporation of the effects of radiation therapies (RTs) (both external and internal) into the previous model;
- endowing the above RT-aware model with capabilities allowing for a simultaneous action of RT and drugs;
- illustration of the RT influence upon oncogenic hyperplasia with computer-simulation results.

Sections 2 and 3 emphasize the key biomedical facts and distinguishing features of living systems to be accounted in the modelling. Sections 4 and 6 presents two parts of the description of the RT-aware model. Sections 5 and 7 discuss the modelling parts in Sections 4 and 6, respectively. The computer-simulation results are described and analyzed in Section 8. Section 9 presents the concluding remarks and suggests a few direction for future research.

2 Biomedical facts to be accounted in the modelling

In order to develop any mathematical model relevant to the hyperplastic tumour formation, a series of biomedical facts should be taken into account. The most important of them are listed below:

- oncogenic hyperplasia is the first stage of any solid tumour development (see Section 1);
- oncogenic hyperplasia is a homeorhetic dysfunction (see Section 1);
- there is no sharp boundary between a tumour and the surrounding population of homeorhetic cells; instead, there is a continuous and complex layer of the cells;
- tumour can be of any shape; it need not be spherical;
- in any spatial domain, the cell population may be at one of the two robust, i.e. asymptotically stable, states: the homeorhesis state that corresponds to a medium-density physical phase of the population and the tumour state that corresponds to a high-density (closest-packed, solid-like) physical phase of the population; which phase is the case in a spatial domain depends on the spatio-temporal distribution of the critical, unstable state;
- oncogenic cells can infinitely proliferate *in vitro* even without a growth-supporting serum, not to mention the nutrient substances necessary for normal cells and the extracellular matrix (ECM) (see Encyclopedia Britannica Online: "Endocrine system: Transforming growth factors");
- as is well known in biomedicine (e.g., [9, 10]), the above proliferation is explained by the autocrine mechanism when, for instance, the transforming growth factor α (TGF-α) molecules bind their corresponding receptors, epidermal growth factor receptors (EGFRs);

None of the above facts can be neglected in the development of meaningful models. They underlie the present model described in the Section 4. The next section discusses the distinguishing features of living systems.

3 Distinguishing features of living systems

The main distinguishing features of the dynamical behaviour of a living system are well known in biology since long ago [2, Chapter 2], [11] (see also [12] for a recent discussion). They are formulated in terms of ordinary differential equations (in Euclidean or function Banach spaces) for the first time in [13, Appendix]. The present section summarizes the latter

consideration and indicates the corresponding reaction-diffusion equation (RDE) applicable to oncogenic hyperplasia.

The aforementioned features are the following.

(i) A living system includes at least one living cell.

(ii) A living system is an open system, i.e. can exchange energy and matter (e.g., cells, molecules, atoms) with the surrounding. Since the system is open, it includes at least one, generally time-varying exogenous (i.e. environmentally driven) signal.

(iii) A living system develops along the trajectory (in the space of the system states) that is completely determined by the internal properties of the system and its environment, i.e. the related exogenous signals.

(iv) The trajectory called *creode* (the necessary route or path) [2, p. 32] corresponds to the "most favored" exogenous signals [2, p. 19]. The latter are also known as the formative drives (according to Aristotle's theory of epigenesis).

(v) The actual trajectory, i.e. the one corresponding to the actual rather than "most favored" exogenous signals, need not be the creode, but in the course of time tends to the latter, no matter what the signals are (in a certain, system-relevant range). This "stability" with respect to the exogenous signals is known as *homeorhesis* [2, p. 32]. (Homeorhesis is the time-dependent generalization of homeostasis. The latter term was coined by W. B. Cannon in 1926 who discussed homeostasis in detail later [14].

One usually associates dynamics of any living system with the *purposeful* behaviour, however, without suggesting the corresponding "mechanism" or specifying the terms. Resolving the latter problem is substantially contributed by Waddington's theory of homeorhesis. Indeed, it follows from feature (v) that the homeorhetic "mechanism" indicates the creode trajectory (which is independent on the actual exogenous signal) as the "purpose" of a living system. This purpose is not invariable: its evolution is described with the creode dynamics.

Remark 3.1 *Exogenous signals are parameters of the environment of a living system but are not parts of the system. They vary in time smoothly and are independent of the moments* $t_{\rm B}$ *and* $t_{\rm D}$ *(*$t_{\rm B} < t_{\rm D}$*) of the birth and death of the system.*

We denote an exogenous signal with $s(t)$ and regard it as a vector in the k-dimensional Euclidean space, i.e. $s(t,x) \in \mathbb{R}^3$ where $x = (x_1, x_2, x_3)^{\rm T} \in \mathbb{R}^k$ and $k \geq 1$. In view of Remark 3.1, $s(\cdot, x) \in B_{\rm k}$ where $B_{\rm k}$ is the set of the functions which have values in $\mathbb{R}^{\rm k}$, and are defined, sufficiently smooth, and uniformly bounded in the *entire* time axis $\mathbb{R}$. We also denote the "most favored" exogenous signal (or formative drive) mentioned in feature (iv) with $s_{\rm c}(t,x)$. It need not coincide with actual exogenous signal $s(t,x)$ and hence is, generally speaking, hypothetical. As explained in [13, the text below (A.11)], it is "designed" by the living system itself and is related to what is in biology known as "the wisdom of the body" (cf., [14]).

Waddington (see [2, p. 22]) suggested to regard the state-space of a living system as Euclidean space, say, $\mathbb{R}^{\rm n}$ ($n \geq 1$) and to describe the system with an ODE of a fairly general form in $\mathbb{R}^{\rm n}$. The coordinates in the state space can include, for instance, concentrations (or volumetric number densities) of cells or molecules [2, Chapter 2 and Appendix].

Let m be the so-called *scaled* concentration of the cells in a population (e.g., [7, 8, 6], see also (2) below). Note that $m > 0$ because of feature (i). Let also $m_{\rm c}$ be the creode value of m. The simplest space-time model for morphogeny is an RDE (e.g., see [6, Section 10] for a recent discussion). Assume that concentration m is described with an RDE where the diffusion coefficient D of a cell is space-time-independent. Then it follows from the results of [13, Appendix] that the RDE can be of the following form

$$\begin{aligned} \frac{\partial[m - m_{\rm c}(t,x)]}{\partial t} &= D\nabla^{\rm T}\nabla[m - m_{\rm c}(t,x)] \\ &+ \Phi(m_{\rm c}(t,x), s(t,x), m)[m - m_{\rm c}(t,x)]\,, \quad x \in \mathbb{R}^3\,,\ t > 0\,, \end{aligned} \tag{1}$$

where column ∇ is the Hamilton differential expression in the spatial coordinates x_1, x_2, and x_3, i.e. $\nabla = (\partial/\partial x_1, \partial/\partial x_2, \partial/\partial x_3)^{\mathrm{T}}$, Φ is certain sufficiently smooth function of respective variables, and m_{c} is uniformly bounded for *all* $t \in \mathbb{R}$. Equation (1) can be regarded as the equation not only for the scaled cell concentration m but also for the cell concentration n (see (2) below). The corresponding NRDE for n (e.g. [7, Appendix B]) is a description of homeorhesis in the particular case when the sensitivity of n with respect to the exogenous signals has already decayed to zero (cf., [13, (A.6) and Theorem A.1]), and therefore the term which represents the above sensitivity is not accounted explicitly. However, its resulting influence upon m is represented with the initial condition (see (10) below).

Note that the creode value $m_{\mathrm{c}}(t, x)$ is uniformly bounded for all t [13, Appendix]. Further details on the differential-equation solutions uniformly bounded for all t can be found in [15]. In theory of Markov stochastic processes, *invariant* (generally, nonstationary) processes (e.g., [16]) are analogues of the above solutions of determinate differential equations.

The advantage of description (1) is that it does not presume to model creode concentration m_{c}: the latter can be obtained from the corresponding experimental data (e.g., see [17] for examples of these data). Function Φ is derived independently of the creode modelling in [6] within the PhasTraM approach. The PhasTraM form of (1) is discussed in Section 4.

4 Model description

The PhasTraM model of [6] (see also [7, 8]) allows for an insight into the cell proliferation. It describes the space-time evolution of the cell concentration n and the cell-population transitions between the two phases noted in Section 2. These phases correspond to the creode concentration n_{c} and the hyperplastic-tumour concentration n_{T}. Between these asymptotically stable values there must be a concentration value which is unstable and, thus, critical. It is denoted with $\overline{n}$. The PhasTraM model extends the well-known theory of the first- and second-order non-equilibrium phase transitions due to chemical reactions [18].

We denote with subscript "$\times$" the values of respective variables corresponding to the case when RT is not applied, i.e. $r \equiv 0$. In the present work the term "parameter" is only applied to the characteristics which are independent of concentrations of cells or molecules.

The PhasTraM model [6] applies the so-called scaled concentration (see [6, Section 2])

$$m = n/(1 - \phi - \Upsilon n)\,, \tag{2}$$

where Υ is the *effective* volume of a cell and ϕ is the volume fraction occupied by bodies of ECM which can be regarded as immobile. Note that ϕ does not include the fibres that may be located within the effective volume. Parameter Υ is defined as $\Upsilon = \upsilon/\zeta$ where υ is the actual volume of the cell and ζ is the ratio of the fraction of the volume occupied by the bodies of the cells to the fraction of the volume unavailable to the cell motion, $\zeta \in (0, 1]$ (for hard spheres $\zeta \approx 0.75$). It follows from (2) that

$$n = [\Upsilon m/(1 + \Upsilon m)]n_{\mathrm{T}}\,, \quad 0 \le n < n_{\mathrm{T}}\,, \tag{3}$$

where

$$n_{\mathrm{T}} = (1 - \phi)/\Upsilon\,. \tag{4}$$

The equation describing the space-time evolution of m is the NRDE of work [6] extended with the RT-term r, namely

$$\begin{aligned} \frac{\partial(m - m_{\mathrm{c}})}{\partial t} &= D\,\nabla^{\mathrm{T}}\nabla(m - m_{\mathrm{c}}) \\ &+ \left(\frac{1}{\eta_\times}\frac{m - \overline{m}_+}{c_\times\, m + \overline{m}_+} - r\right)(m - m_{\mathrm{c}}), \quad x \in \mathbb{R}^3,\ t > 0, \end{aligned} \tag{5}$$

where $\overline{m}_+$ is explained below (see (21)), D is the diffusion coefficient of a cell, the last term on the right-side is the biochemical-reaction (BCR) term, $\eta_\times$ is the lifetime of a cell in the ideal-homeorhesis state $\overline{m}_+ = \infty$,

$$\eta_\times = \xi_\times/\ln 2\,, \tag{6}$$

$m_{\rm c}$ is the creode value of m (see Section 3), $\overline{m}_+$ is the critical value of m, r is the rate of cell death caused by RT,

$$r = u + \kappa\, n_{\rm I}, \tag{7}$$

and $c_\times$ is determined as follows

$$c_\times = (\xi_\times + \theta_\times)/(\eta_\times \ln 2) = (3 - g_\times)/(1 + g_\times)\,. \tag{8}$$

In the above formulas, $\xi_\times$ is the total duration of the S and M cell-cycle stages, $\theta_\times$ is the total duration of the G1 and G2 cell-cycle,

$$\theta_\times = 2\,\xi_\times(1 - g_\times)/(1 + g_\times)\,, \tag{9}$$

$g_\times$ is the genotoxicity of a cell, u is a rate of decrease of m due to the external RT, κ is a coefficient related to the internal RT and $n_{\rm I}$ is a concentration of the radioactive substance used in the internal RT.

For the reasons noted in the text below (1), we consider the initial condition for (5), namely

$$\lim_{t\downarrow 0} m = m_0(x), \qquad x \in \mathbb{R}^3, \tag{10}$$

where initial scaled concentration m_0 is coupled with initial concentration n_0 by means of (3). Values $n_0(x)$ are obtained from the related experiments.

As it is shown in Appendix A.1, equation (5) can be presented in the more concise form, namely

$$\begin{aligned} \frac{\partial(m - m_{\rm c})}{\partial t} &= D\,\nabla^{\rm T}\nabla(m - m_{\rm c}) \\ &+ \frac{1}{\eta}\frac{m - \overline{m}}{c\,m + \overline{m}}(m - m_{\rm c}), \quad x \in \mathbb{R}^3,\ t > 0, \end{aligned} \tag{11}$$

where

$$\overline{m} = \overline{m}_+(1 + r\eta_\times)/(1 - r\eta_\times c_\times)\,, \tag{12}$$

$$\eta = \eta_\times/(1 + r\eta_\times)\,, \tag{13}$$

$$c = c_\times\,(1 + r\eta_\times)/(1 - r\eta_\times c_\times)\,. \tag{14}$$

Since the form of (11) is the same as that of the NRDE studied in [7, 8, 6], the analytical results of these works are applicable. They include the following relations:

$$c = (\theta + \xi)/(\eta \ln 2)\,, \quad c \in [1, 3)\,, \tag{15}$$

$$g = (3 - c)/(1 + c)\,, \quad g \in (0, 1]\,, \tag{16}$$

$$0 \le \theta/\,\xi < 2\,, \tag{17}$$

$$\overline{m} = \frac{c(1 + c)}{3 - c}\, m_{\rm c}\,. \tag{18}$$

Appendix A.2 shows how the durations of the cell-cycle stages depend on applied radiation

$$\xi = \xi_\times/(1 - r\eta_\times c_\times)\,, \tag{19}$$

$$\theta = \theta_\times/(1 - r\eta_\times c_\times)\,. \tag{20}$$

Another necessary relation

$$\overline{m}_+ = \frac{c_\times(1 + c_\times)}{3 - c_\times(1 + 4r\eta_\times)}\, m_{\rm c}\,, \tag{21}$$

is derived in Appendix A.3. Expression (see Appendix A.4)

$$\xi/(\eta \ln 2) = c/c_\times \tag{22}$$

generalizes (6) to the case when r need not be identically equal to zero. Inequalities (17) agrees with the corresponding experimental data (e.g., [19, p. 926]). Inequality

$$\overline{m} < m \tag{23}$$

is interpreted as the threshold that prevents the cells from entering the G0 stage of the cell cycle, thereby transferring them into the nonquiescent ones.

Remark 4.1 *The present model presumes that cell genotoxicity* $g_\times$ *(see (9))*

$$g_\times = (2\,\xi_\times - \theta_\times)/(2\,\xi_\times + \theta_\times)\,,$$

depends on space and time and, in the course of time, can rapidly change from low to high values (and back) thereby (see (8), (21), and (12)) providing the switching $\overline{m}$ *between high and low values. When inequality (23) holds, oncogeny begins. It lasts as long as the inequality is valid. When it is no longer valid, a resulting hyperplastic tumour disintegrates.*

The above results enable one to derive expression (see Appendix A.5)

$$g = (1 + r\eta_\times)g_\times - 3r\eta_\times \tag{24}$$

and inequalities (see derivation in Appendix A.6)

$$3r\eta_\times/(1 + r\eta_\times) < g_\times \le (1 + 3r\eta_\times)/(1 + r\eta_\times)\,. \tag{25}$$

The first inequality in (25) is equivalent to

$$r = u + \kappa\, n_{\rm I} < \frac{1}{\eta_\times}\frac{g_\times}{3 - g_\times}\,. \tag{26}$$

Remark 4.2 *Relation (26) is a specific quantitative criterion to design and plan RTs. It can serve as a guidance to optimize the settings for the intensity-modulated RT (IMRT) technique (e.g., [20]) or to determine the space-time dependence of* $n_{\rm I}$ *used by an internal RT (see for more details Section 5).*

Since the x-domain in (5) is the entire space $\mathbb{R}^3$, the initial-value problem (11), (10) is the Cauchy one. An analytical-numerical time-slices (TS) method to solve this problem is available (see [6, Appendix C] or [21, 22]). The key advantages of the TS method are that it is applicable to nonlinear RDEs, equally efficient in simulation of both asymptotically stable solutions (i.e. when $m \to m_{\rm c}$) and unstable solutions (i.e. when $m \to \infty$), and is sufficiently fast to provide efficient multiple analysis.

Remark 4.3 *In the present model, creode concentration* $m_{\rm c}$ *is assumed to be independent of the RT-related rate* $r \ge 0$ *(see (7)). This in particular results in inequality (26). In other words, the sufficiently low values of* r *prescribed by (26) corresponds to the* r*-independence of* $m_{\rm c}$*. Thus, the higher values of* r *can be the case only if the creode is affected by RT.*

However, in view of the meaning of the creode (see Section 3), the creode alteration by RT may cause iatrogenic diseases thereby changing the status of the RT treatment from a therapy to something which is probably opposite to therapy. The iatrogenic effect of RT as well as the related biomedical, ethical, and legal issues are beyond the scope of this work.

Other terms related to the above model (see (11)) are introduced in Section 6.

5 Discussion of the model in Section 4

The model of the previous section applies the initial value of the cell scaled concentration m_0 resulting from input parameter n_0 by means of (3). Since the model describes a spatially growing tumour, n_0 must be a function of the space point. The present measurements *in vivo* do not resolve the cell concentration in space. Nevertheless, it is possible to make approximate characterization of the shape of n_0 on the basis of several point biopsies. In the clinical practise, a widely used procedure for obtaining cytological parameters at a location of interest to physicians is the fine needle aspiration biopsy (FNAB). It is, in contrast to surgical biopsy, safer and less traumatic for the patient. The FNAB procedure is frequently performed in breast, thyroid, lung, upper abdomen, kidney and bone marrow studies. In order to ensure the appropriate accuracy, the stereotactic needle biopsy is performed, a biopsy in which the spot is located three-dimensionally by means of ultrasound, MR or CT imaging.

The model in Section 4 includes relations for certain characteristics of the cells, such as (13), (19) and (20), which depend on r. The r-dependences in (19) and (20) qualitatively agree with what is known from the phenomenological description of the RT influence on the cell cycle (e.g., [23]). The advantage of mathematical modelling is the possibility to predict the cell-related effects not only after application of RT but also at a time when RT is applied.

Inequality (26) gives a consistent and specific recipe for designing the shape of r. The r should, however, be close to the right-hand side of (26) as much as possible. This quantitative description can be used as an additional factor for the planning RT, also in such an advanced method as like IMRT.

6 The TGF-α/EGFR interpretation of the present model

The BCR term in NRDE (11) is a rational function of m. This form can be explained in terms of the interaction of the TGF-α molecules with EGFRs in the following way.

One considers equation system more general then NRDE (11), namely

$$\frac{\partial(m-m_{\rm c})}{\partial t} = D\,\nabla^{\rm T}\nabla(m-m_{\rm c}) + (p+q\nu)(m-m_{\rm c}), \tag{27}$$

$$\frac{\partial \nu}{\partial t} = D_\nu \nabla^{\rm T}\nabla\nu - \frac{1}{\tau}\,\nu + am(\nu_{\rm T}-\nu), \tag{28}$$

where p and q are the coefficients to be determined, ν is the TGF-α molecule concentration, D_ν is diffusion coefficient of a TGF-α molecule, τ is the lifetime of a TGF-α molecule, a is the autocrinity of a cell and $\nu_{\rm T}$ is the value of ν corresponding to $n_{\rm T}$. The gain term $am\nu_{\rm T}$ on the right-hand side of (28) describes the production of TGF-α molecules by the cells, and the loss term $-am\nu$ describes the decrease in TGF-α molecules due to their binding by the cells.

Remark 6.1 *Parameter τ can include various effects. For instance, the effect of the TGF-α-molecule-deactivating drug can be accounted in the following expression*

$$\tau^{-1} = \tau_0^{-1} + \omega n_{\rm II}\,, \tag{29}$$

where $n_{\rm II}$ is the concentration of the drug, τ_0 is the value of τ at $n_{\rm II}=0$, and $\omega \geq 0$ is the corresponding coefficient. In general, the specific expressions for τ depend on specific problems.

Involving the quasi-stationary approximation in (28), i.e. neglecting all the derivatives in (28), one obtains expression (see the derivation in Appendix B.1)

$$\nu = \frac{(g/m_{\rm c})\,m}{1+(g/m_{\rm c})\,m}\,\nu_{\rm T}\,, \tag{30}$$

where g is described with (24).

The coefficients p and q in (27) should be selected in such a way that, after substituting (30) into (27), one arrives with (11). Incorporation p and q into (27) leads to more detailed expression (see derivation of (B.4) and (B.6) in Appendix B.1 for p and q, respectively)

$$\frac{\partial(m-m_{\rm c})}{\partial t} = D\,\nabla^{\rm T}\nabla(m-m_{\rm c}) + \frac{1}{\eta}\big(-1+\frac{\nu}{\overline{\nu}}\big)(m-m_{\rm c})\,, \tag{31}$$

where $\overline{\nu}$ is the value of ν that corresponds to $\overline{m}$. As it is shown in the part of the text in Appendix B.1 on the derivation of the BRC coefficient in (31), quantity $\overline{\nu}$ has the following form

$$\overline{\nu} = \nu_{\rm T}\,c/(1+c)\,. \tag{32}$$

It is possible to derive another expression for g (see Appendix B.1), namely

$$g = \tau\,a\,m_{\rm c}\,. \tag{33}$$

This relation explains genotoxicity g by means of autocrinity a and the TGF-α-molecule lifetime τ, both are the kinetic parameters.

The RT-free version of (33) is

$$g_\times = \tau a_\times m_\mathrm{c}\,. \tag{34}$$

Subsequently, the coupling of a and $a_\times$ is similar to that of g and $g_\times$ (see (24)).

Remark 6.2 *Equations (33) and (24) (see also (9)) present an* explicit analytical *connection between the cell-cycle parameters $\theta_\times$ and $\xi_\times$, on the one hand, and kinetic parameters a and τ, on the other hand. This coupling, expressed explicitly, points out the cell-phenomena connection that has not been revealed before.*

A furter analysis of the model leads to an expression for ν_T which depends on parameter (38) and ν_c (see Appendix B.2 for the derivation),

$$\nu_\mathrm{T} = \frac{1+g_\mathrm{c}}{g_\mathrm{c}}\,\nu_\mathrm{c}\,. \tag{35}$$

As it is well known from experiments (e.g. [24, Figure 8(B)]), the dependence of n (see (3)) on ν (see (30)) is linear. Such dependence straightforwardly results in relation

$$\Upsilon = g/m_\mathrm{c} \tag{36}$$

if one assumes that the linearity is the case even if RT is applied. Note that the cell effective volume Υ is never less than the cell volume v and is equal to the latter at the creode state, i.e.

$$\Upsilon \geq \Upsilon\big|_{g=g_\mathrm{c}} = v\,. \tag{37}$$

This and (36) in particular show that

$$g_\mathrm{c} = v m_\mathrm{c}\,. \tag{38}$$

On the basis of (36), one can obtain the following equations (see Appendixes B.3 and B.4 for the derivation of (39) and (40), (41), respectively)

$$n_\mathrm{T} = \frac{1+vm_\mathrm{c}}{vm_\mathrm{c}}\,n_\mathrm{c}\,, \tag{39}$$

$$m_\mathrm{c} = \frac{n_\mathrm{c}}{v(n_\mathrm{T}-n_\mathrm{c})}\,, \tag{40}$$

$$\phi = 1-\frac{n_\mathrm{T}}{m_\mathrm{c}}\,g\,. \tag{41}$$

Value n_T is derived in Appendix B.4.

The present model is discussed in the next section.

7 Discussion of the model in Section 6

In the present model genotoxicity g is a function of τ and a (see (33)). Nevertheless, when those parameters are unavailable, g can be calculated by means of parameters of the cell-cycle duration (see (24) and (9)). Quantity τ in (33) can easily be obtained from the measurements of the lifetime of TGF-α molecules in the surrounding where the cells are not present. An obtaining autocrinity a in (33) seams to be more complicated. A model for a is to be developed. This model should describe the interaction of TGF-α molecules and their receptors at the cell surface, as well as the production of the molecules by the cells. The molecule-receptor binding may be rather complex.

Since ϕ is the volume fraction occupied by the ECM part located beyond the effective volume of a cell, relation (41) describes the ECM degradation at growing genotoxicity g, the phenomenon is closely associated with oncogenic fibroplasia. The latter may be performed also within the effective cell volume Υ. This means that the present model includes a concise fibroplasia description complementing the autocrine origin of oncogeny. The mentioned coupling is in line with, and further develops, the well-known modelling vision reported in [25].

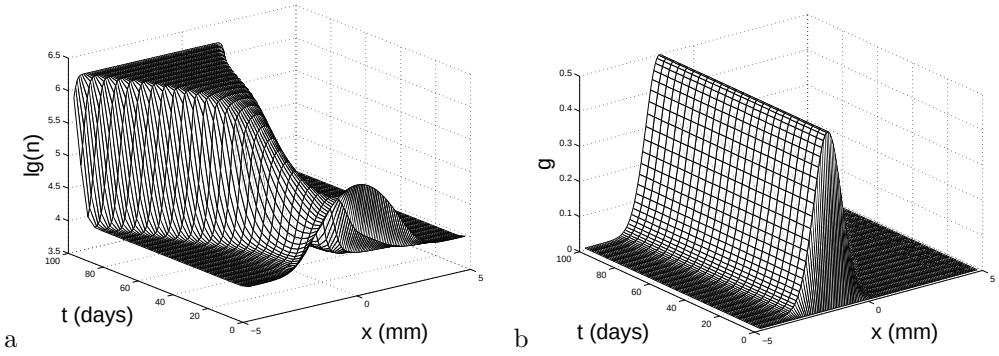

Figure 1: Hyperplastic tumour formation case: (**a**) time-space surface of the cell concentration n (mm^{-3}); (**b**) time-space surface of the genotoxicity g.

8 Examples of numerical results

The time-slices (TS) method described previously in [6, Appendix C], [21, 22] was implemented in a simulation software within the MATLAB environment. The current version of the software enables a time-dependent simulation in one spatial dimension with incorporation of the RT action. Note that the TS method has been derived for the general case of three spatial dimensions.

This section describes four examples. The first and second examples do not include the action of RT (r is assumed to be 0). They are shown in the time-space domain $(t, x) \in [0, 100] \times [-5, 5]$ days $\times$ mm (see Figures 1 and 2). The other two examples which include the RT action are shown in the time-space domain $(t, x) \in [0, 90] \times [-6, 6]$ days $\times$ mm (see Figures 3 and 4). The cell genotoxicity $g_\times(t, x)$ is used as an input parameter. (The after-growth drop in it may represent the action of, for instance, the immune system.) Other input parameters for all of the examples are quantified as follows: $\phi = 0.2$, $\upsilon = 5 \times 10^{-7}$ mm^3, $\xi_\times = 1$ day, $D = 0.01$ mm^2/day, and $n_\mathrm{c}(t, x) = 10^4$ mm^{-3}. Initial concentration $n_0(x)$ (see the text below (10) and Section 5) is assumed to be the sum of n_c and the "bell"-shaped deviation from n_c (see the data in Figure 1-4(a) at $t = 0$). The shape of the $g_\times(t, x)$ surface for the second example is shown in Figure 2(b). In the other examples, the $g_\times(t, x)$ surface has the shape presented by Figure 1(b). For first two examples, $r = 0$ and $g_\times = g$. The shapes of g for the next two examples, where $r \neq 0$, are presented in Figures 3(b) and 4(b), respectively.

Figure 1(a) shows the changes of the cell concentration $n(t, x)$ corresponding to $g(t, x)$ in Figure 1(b). As one can see, n decreases down to the creode value $n_\mathrm{c}(t, x)$ during a short time and then, because of the increase in $g(t, x)$, begins to grow, and, in the time limit, tends to the tumour value n_T thereby forming a tumour. The tumour value is determined with the equality in Appendix B.4, specifically, $n_\mathrm{T} = 1.6 \times 10^6$ mm^{-3} ($\lg n_\mathrm{T} \approx 6.2$). The tumour is formed since the cell genotoxicity $g(t, x)$ keeps a sufficiently high value represented with the top of the "ridge" in Figure 1(b) (cf., Remark 4.1).

In the second example (see Figure 2), the cell genotoxicity $g(t, x)$ keeps a high value during a short time interval only (see Figure 2(b)). As a result (see Figure 2(a)), the cell concentration n does not continue to tend to the value n_T (cf., Figure 1(a)) but, due to the decrease in $g(t, x)$ in the course of time, begins to drop down to the creode value n_c, as it should be (see Remark 4.1).

The third and fourth examples examine the influence of RT on the growth dynamics of the cell population. As it is discussed in Section 5, the closer r is to the value of the right-hand side of (26) the more effective RT is. To study a mere manifestation of the RT effect, it is sufficient to use some constant parameter γ, which characterizes the effectiveness of RT (cf. (26)), namely

$$r = \gamma \, \frac{1}{\eta_\times} \frac{g_\times}{3 - g_\times} \,, \quad \gamma \in [0, 1) \,.$$

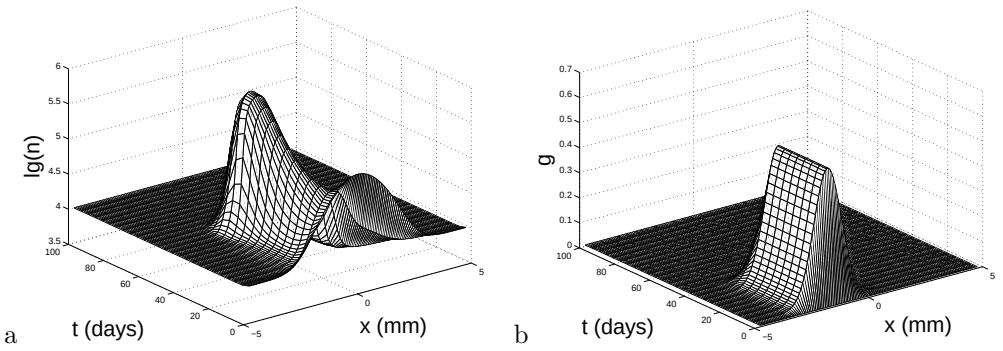

Figure 2: Tumour disintegration case: (**a**) time-space surface of the cell concentration n (mm^{-3}); (**b**) time-space surface of the genotoxicity g.

In the present examples, we used $\gamma = 0.93$.

Figure 3(a) shows the changes in cell concentration $n(t,x)$ corresponding to $g(t,x)$ (see Figure 3(b)). The drop of the value of $g(t,x)$ is due to the action of RT. The decrease in $g(t,x)$ results in the decrease in the cell concentration (see Figure 3(a)). The later return of $g(t,x)$ to its maximum value leads to a continuous growth of $n(t,x)$ resulting in the limit tendency to n_{T}. Figure 3(c) presents the cross-sections through the n_{c}, n, $\overline{n}$, and n_{T} surfaces. The cross-section abscissa corresponds to the maximum-in-x values of n along the t-axis. The change in the profile of $\overline{n}$ (see dot-dashed line) is due to the action of RT. The "switching" character of $\overline{n}$ is easily seen in this figure.

The last example (see Figure 4) presents a successful application of RT, i.e. the one leading to disintegration of the tumour. Figure 4(a) shows cell concentration $n(t,x)$ and Figure 4(b) shows the corresponding $g(t,x)$ function. The longer action of RT, namely for 3 days greater then in previous example, is presented with the longer "gap" in the shape of $g(t,x)$ and is sufficient to suppress the tumour growth. Figure 4(c) with the cross-sections through the n_{c}, n, $\overline{n}$, and n_{T} surfaces illustrates the suppression because $\overline{n}$ does not intersect n.

The aforementioned examples explicitly demonstrate the main capabilities of the model developed in Sections 4 and 6. The next section summarizes and concludes the work.

9 Concluding remarks and directions for future research

Summing up the present work, we note the following two groups of the results which correspond to the purpose formulated in Section 1.

The *first* group of the results is related to the generalization of the oncogenic-hyperplasia model [7, 8, 6, 21] for the effects of both external and internal RTs. The main equations in the resulting model are NRDE (11) and initial condition (10). Other related quantities are described in Sections 4 and 6. The RT-term r (see (7)) includes the external- and internal-RT terms. Moreover, the *explicit analytical* expressions are derived for the influence of the RT-term upon the key characteristics of the cell population such as:

- the ideal-homeorhesis lifetime of a cell (see (13));
- the total duration of the S and M stages of the cell cycle (see (19));
- the total duration of the G1 and G2 stages of the cell cycle (see (20));
- the cell genotoxicity (see (24));
- the critical cell concentration (see (21) and Remark 4.1);
- the cell autocrinity (see (33));

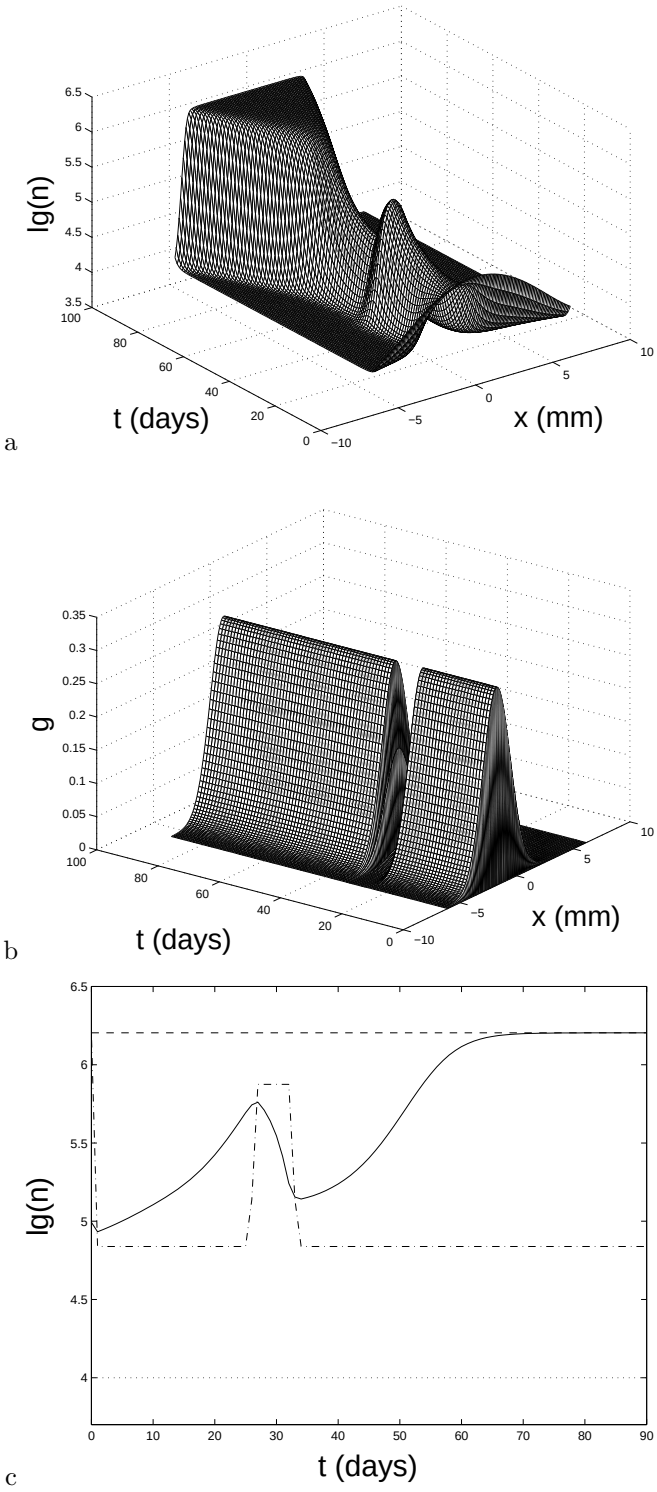

Figure 3: Unsuccessful RT treatment case: (**a**) time-space surface of the cell concentration n (mm^{-3}); (**b**) time-space surface of the genotoxicity g; (**c**) cross-section of the n_{c} (dotted line), n (solid line), $\overline{n}$ (dot-dashed line), and n_{T} (dashed line) surfaces.

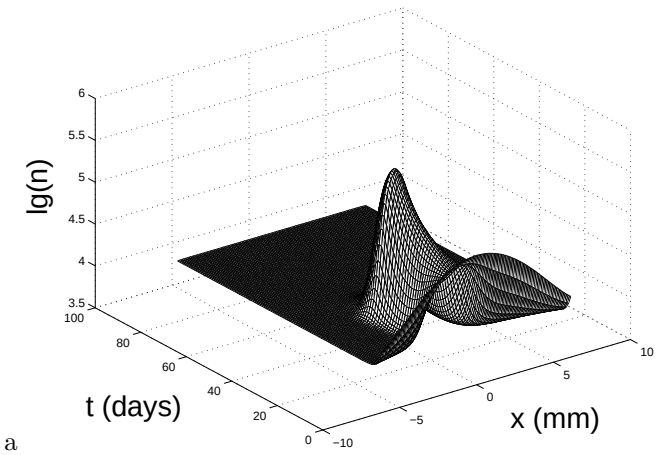

a

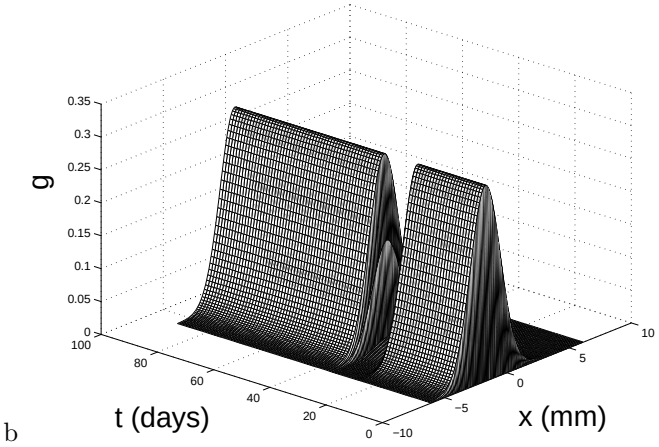

b

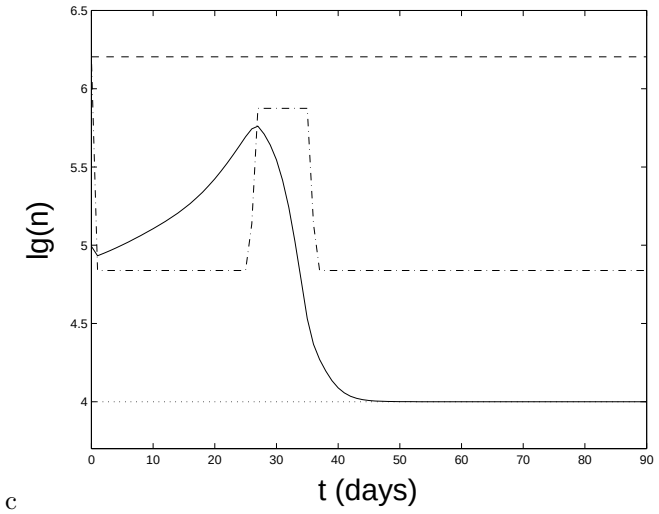

c

Figure 4: Successful RT treatment case: (**a**) time-space surface of the cell concentration n (mm^{-3}); (**b**) time-space surface of the genotoxicity g; (**c**) cross-section of the n_{c} (dotted line), n (solid line), $\overline{n}$ (dot-dashed line), and n_{T} (dashed line) surfaces.

- the oncogeny-caused ECM degradation (see (41)).

Moreover, the explicit analytical results include:

- the *specific quantitative* recipe (26) to design or plan external or internal RTs (see Remark 4.2 for the details; see also Remark 4.3);
- the straightforward connection (by means of the cell genotoxicity g) between the cell-cycle parameters (see (9)), on the one hand, and the cell autocrinity (see (33)), on the other hand (see Remark 6.2 for further details).

The list of the input and output parameters of the above, RT-aware generalization are in Tables 1 and 2, respectively. Each of them has a distinct biomedical meaning.

Table 1: List of Input Parameters

Symbol	Description
υ	volume of a cell
$n_0(x)$	initial concentration of cells
$n_{\rm c}$	creode concentration of cells
D	diffusion coefficient of a cell
$\xi_\times$	sum of the duration of the S and M cell-cycle stages at $r \equiv 0$
$\phi_{\rm c}$	creode value of volume fraction occupied by the ECM
u	rate of the decrease in concentration m due to the external radiotherapy
κ	coefficient related to the internal radiotherapy
$n_{\rm I}$	concentration of a radioactive substance used in the internal radiotherapy
$a_\times$	autocrinity of a cell at $r \equiv 0$ *
τ	lifetime of a TGF-α molecule when there are no cells
$\nu_{\rm c}$	concentration of TGF-α molecules which corresponds to $n_{\rm c}$
ω	coefficient related to TGF-α blocking drug
$n_{\rm II}$	concentration of the drug molecules which bind to the TGF-α molecules preventing the latter from the binding to the cell EGFRs

* because of (34) one can apply $g_\times$ as an input parameter instead of $a_\times$; if so, $g_\times$ can be evaluated from (9) on the basis of the data for $\xi_\times$ and $\theta_\times$

The *second* group of the results of the work is associated with the fact that the developed model includes the action of the drug molecules which deactivate the TGF-α molecules by binding to them. This is presented with the drug-molecule concentration $n_{\rm II}$ and coefficient ω in (29). The latter, together with (24) and (9), explicitly shows how the above deactivation affects the genotoxicity of a cell and the cell-cycle parameters. The TGF-α-deactivating drug can be used in conjunction with RT, thereby improving the effect of the latter.

The developed model and related results draw attention to various directions for future research. We mention a few of them.

- Specification of the RT term r (see (7)) by means of the input physical parameters common to the end users.
- Coupling of the modelling/simulation with the corresponding experimentally available data for the cell-cycle parameters employed in (9).
- Incorporation of the autocrinity model as well as the aforementioned RT-term r (see (7)) and the TGF-α-deactivating-drug terms into the present software. This presumes application of the related numerical-simulation results to the RT-design/planning recipe (26). In so doing, g can come from either (9) or (33), whereas other parameters are extracted from experiments.
- Validation of the model and calibration of its parameters on the basis of the available *in vivo* measurements.

Table 2: List of the Main Output Parameters

Symbol	Description
n	concentration of cells
m	scaled concentration of cells
ν	concentration of TGF-α molecules
m_{c}	homeorhetic scaled concentration of cells
n_{T}	tumour value of n
$\overline{n}$	critical value of n
$\overline{m}$	critical value of m
g	genotoxicity of a cell
c	auxiliary parameter which is in a one-to-one correspondence to g
ξ	sum of the duration of the S and M cell-cycle stages
θ	sum of the duration of the G1 and G2 cell-cycle stages
η	homeorhesis lifetime of a cell
$g_{\times}$	value of g at $r \equiv 0$
$c_{\times}$	value of c at $r \equiv 0$
$\theta_{\times}$	value of θ at $r \equiv 0$ ($\theta_{\times}$ is output parameter only if both $a_{\times}$ and τ are input parameters (see the footnote in Table 1))
$\eta_{\times}$	value of η at $r \equiv 0$
ν_{T}	value of ν which corresponds to n_{T}
Υ	effective volume of cells
ϕ	volume fraction occupied by the extracellular matrix

- Incorporation of a model of oncogenic fibroplasia (e.g., [25]) that will provide a *combined*, hyperplastic-fibroplastic description. (The latter will noticeably generalize the present, quite concise representation (41) for the ECM degradation.)
- Development of the software version that will provide the simulation for two-dimensional spatial domains.

The proposed model, *minimal* but fairly capable, can be regarded as a specific theoretical, mathematical and computer-simulation tool in *tackling complexity in oncology* by means of a cohesive multidisciplinary efforts. The main applications of the model are:

- planning external or internal RTs with the subsequent, or even simultaneous, use of the TGF-α-deactivating drugs;
- preclinical testing new antitumour drugs that would substantially reduce the risk of extremely costly failures at the late phases of clinical trails;
- quantitative research of oncogenic hyperplasia in cancer and other proliferative diseases.

Future applications of the present model will allow to specify many still unclear features of oncogenic hyperplasia and help to discover ways to prevent the disease of at least five-thousand-year history.

Acknowledgements

The authors thanks the European Commission Marie Curie Research Training Network MRTN-CT-2004-503661 "Modelling, Mathematical Methods and Computer Simulation of Tumour Growth and Therapy" (http://calvino.polito.it/∼mcrtn/) for the full support of the first author. It is a pleasure of the authors to express their gratitude to E. Forssell-Aronsson, Department of Radiophysics, Göteborg University and Sahlgrenska University Hospital (Göteborg, Sweden) and L. Preziosi, Dipartimento di Matematica, Politecnico di Torino (Turin, Italy) for fruitful discussions and stimulating remarks on the research reported in the present work. The authors are also grateful to D. Hanstorp and L. Sjögren, Prefect and Research Proprefect, respectively, Department of Physics, Göteborg University (Göteborg, Sweden) for their attention to the present research and encouragement.

Appendix A
Derivations of equations from Section 4

A.1 Derivation of the reaction coefficient in (11)

In order to obtain (11) from (5), one follows the derivation below

$$\begin{aligned}
\frac{1}{\eta_\times}\frac{m-\overline{m}_+}{c_\times\, m+\overline{m}_+} - r &= \frac{m-\overline{m}_+ - r(\eta_\times c_\times\, m+\eta_\times\overline{m}_+)}{\eta_\times c_\times\, m+\eta_\times\overline{m}_+} \\
&= \frac{m(1-r\eta_\times c_\times)-\overline{m}_+(1+r\eta_\times)}{\eta_\times c_\times\, m+\eta_\times\overline{m}_+} \\
&= \frac{(1-r\eta_\times c_\times)(m-\frac{1+r\eta_\times}{1-r\eta_\times c_\times}\,\overline{m}_+)}{\eta_\times c_\times\, m+\eta_\times\overline{m}_+} \\
&= \frac{m-\frac{1+r\eta_\times}{1-r\eta_\times c_\times}\,\overline{m}_+}{\frac{\eta_\times}{1-r\eta_\times c_\times}c_\times\, m+\frac{\eta_\times}{1-r\eta_\times c_\times}\overline{m}_+} \\
&= \frac{m-\frac{1+r\eta_\times}{1-r\eta_\times c_\times}\,\overline{m}_+}{\frac{\eta_\times}{1+r\eta_\times}\frac{1+r\eta_\times}{1-r\eta_\times c_\times}\,c_\times\, m+\frac{\eta_\times}{1+r\eta_\times}\frac{1+r\eta_\times}{1-r\eta_\times c_\times}\,\overline{m}_+} \\
&= \frac{1}{\eta}\frac{m-\overline{m}}{c\,m+\overline{m}}\,.
\end{aligned}$$

The latter equality shows that $\overline{m}$, η, and c are represented by (12), (13) and (14), respectively.

A.2 Derivation of (19), and (20)

Substituting (8) into (14), one achieves

$$\begin{aligned}
c &= \frac{1+r\eta_\times}{1-r\eta_\times c_\times}\,c_\times \\
&= \frac{1+r\eta_\times}{1-r\eta_\times c_\times}\,\frac{\xi_\times+\theta_\times}{\eta_\times\ln 2} \\
&= \left(\frac{\xi_\times}{1-r\eta_\times c_\times}+\frac{\theta_\times}{1-r\eta_\times c_\times}\right)\frac{1+r\eta_\times}{\eta_\times\ln 2}\,,
\end{aligned}$$

that, because of (15), results in (19) and (20).

A.3 Derivation of (21)

Derivation of $\overline{m}_+$ begins from (12) where value $\overline{m}$ is expressed by (18). Thus,

$$\overline{m}_+ = \frac{1-r\eta_\times c_\times}{1+r\eta_\times}\,\frac{c(1+c)}{3-c}\,m_{\mathrm{C}}\,. \tag{A.1}$$

Application of (14) to (A.1) leads to

$$\begin{aligned}
\overline{m}_+ &= c_\times\,\frac{1+c_\times(\frac{1+r\eta_\times}{1-r\eta_\times c_\times})}{3-c_\times(\frac{1+r\eta_\times}{1-r\eta_\times c_\times})}\,m_{\mathrm{C}} \\
&= c_\times\,\frac{1-r\eta_\times c_\times+c_\times(1+r\eta_\times)}{3(1-r\eta_\times c_\times)-c_\times(1+r\eta_\times)}\,m_{\mathrm{C}} \\
&= \frac{c_\times(1+c_\times)}{3-c_\times(1+4r\eta_\times)}\,m_{\mathrm{C}}\,.
\end{aligned}$$

The latter equality presents (21).

A.4 Derivation of (22)

Relation (14) is equivalent to

$$\frac{c}{c_\times} = \frac{1 + r\eta_\times}{1 - r\eta_\times c_\times}\,,$$

where the numerator and the denominator can be substituted by (13) and (19), respectively. This result in

$$\frac{c}{c_\times} = \frac{\eta_\times}{\eta}\,\frac{\xi}{\xi_\times}\,,$$

that, in view of (6), leads to (22).

A.5 Derivation of (24)

Substituting (14) into (16), one obtains g as a function of $c_\times$, namely

$$\begin{aligned} g &= \frac{3-c}{1+c} \\ &= \frac{3(1-r\eta_\times c_\times) - c_\times(1+r\eta_\times)}{1 - r\eta_\times c_\times + c_\times(1+r\eta_\times)} \\ &= \frac{3 - c_\times(1+4r\eta_\times)}{1+c_\times}\,. \end{aligned} \tag{A.2}$$

In view of (8), (A.2) is transformed into

$$\begin{aligned} g &= \frac{3(1+g_\times) - (3-g_\times)(1+4r\eta_\times)}{1+g_\times+3-g_\times} \\ &= \frac{4g_\times - 12r\eta_\times + 4r\eta_\times g_\times}{4} \\ &= g_\times(1+r\eta_\times) - 3r\eta_\times\,. \end{aligned}$$

The latter equality is (24).

A.6 Derivation of (25)

As it is noted in (16), $0 < g \le 1$. Applying (24) to the latter relation, one obtains

$$0 < g_\times(1+r\eta_\times) - 3r\eta_\times \le 1\,,$$

which, after simple manipulations, is transformed into the form (25).

Appendix B
Derivations of equations from Section 6

B.1 Derivation of (30)-(33)

Neglecting all of the derivatives of ν in (28) leads to

$$\begin{aligned} 0 &= -\frac{1}{\tau}\,\nu + am(\nu_{\rm T} - \nu)\,, \\ \nu &= \tau am(\nu_{\rm T} - \nu)\,, \\ \nu &= \frac{\tau am}{1+\tau am}\,\nu_{\rm T}\,. \end{aligned} \tag{B.1}$$

Substituting quasi-stationary approximation (B.1) into the coefficient in the BCR term in (27), one obtains

$$\begin{aligned} p+q\nu &= p+q\frac{\tau\, a\, m}{1+\tau\, a\, m}\,\nu_{\rm T} \\ &= \frac{p+p\,\tau\, a\, m+q\,\tau\, a\, m\,\nu_{\rm T}}{1+\tau\, a\, m} \\ &= \frac{\tau\, a\, m(p+q\,\nu_{\rm T})+p}{\tau\, a\, m+1} \\ &= \frac{\tau\, a\,\overline{m}\, m(p+q\,\nu_{\rm T})+p\,\overline{m}}{\tau\, a\,\overline{m}\, m+\overline{m}}\,. \end{aligned} \tag{B.2}$$

Comparison of the coefficient form (B.2) with the BCR coefficient in (11) gives relations

$$c=\tau\, a\,\overline{m}\,, \tag{B.3}$$

$$p=-1/\eta\,, \tag{B.4}$$

$$c(p+q\,\nu_{\rm T})=1/\eta\,.$$

The latter is equivalent to

$$q=\frac{1+c}{c\,\eta\,\nu_{\rm T}}\,. \tag{B.5}$$

It follows from (B.1) at $m=\overline{m}$ and (B.3) that (32) holds. Substituting (32) into (B.5), one gets the relation for q, namely

$$q=\frac{1}{\eta\,\overline{\nu}}\,. \tag{B.6}$$

Results (B.4) and (B.6) provide the form (31) of RDE (27).

Application of (18) to (B.3) and accounting (16) result in (33), namely

$$c=\tau\, a\,\frac{c(1+c)}{3-c}\,m_{\rm c}\,,$$

$$1=\tau\, a\,\frac{1}{g}\,m_{\rm c}\,.$$

Relation (33) is used in (B.1) to obtain (30).

B.2 Derivation of (35)

It is possible to obtain relation for $\nu_{\rm c}$ from (30) and (38), i.e.

$$\nu_{\rm c}=\frac{(g_{\rm c}/m_{\rm c})\,m_{\rm c}}{1+(g_{\rm c}/m_{\rm c})\,m_{\rm c}}\,\nu_{\rm T}=\frac{\upsilon\, m_{\rm c}}{1+\upsilon\, m_{\rm c}}\,\nu_{\rm T}\,, \tag{B.7}$$

that directly implies relation (35).

B.3 Derivation of (39)

It follows from (3) and (36) that

$$n=\frac{(g/m_{\rm c})\,m}{1+(g/m_{\rm c})\,m}\,n_{\rm T}\,. \tag{B.8}$$

For $n=n_{\rm c}$ the latter takes (see also (38)) the form

$$n_{\rm c}=\frac{(\upsilon m_{\rm c}/m_{\rm c})\,m_{\rm c}}{1+(\upsilon m_{\rm c}/m_{\rm c})\,m_{\rm c}}\,n_{\rm T}=\frac{\upsilon m_{\rm c}}{1+\upsilon m_{\rm c}}\,n_{\rm T}\,, \tag{B.9}$$

that is equivalent to (39).

B.4 Derivation of (40) and (41)

Relation (41) for ϕ is derived from (4) and (36).

The expression to determine n_{T} in (41), i.e. $n_{\mathrm{T}} = (1 - \phi_{\mathrm{c}})/\upsilon$, results from the version of (4) for the creode and the equality in (37). Note that ϕ_{c} is one of the input parameters (see Table 1). Value (40) is obtained from (39) and (37).

References

[1] W.B. Cannon, Organization for physiological homeostasis, Physiol. Rev. 9 (1929) 399–431.

[2] C.H. Waddington, The Strategy of the Genes: A Discussion of Some Aspects of Theoretical Biology, George Allen and Unwin, London, 1957.

[3] O.H. Iversen, Cybernetic aspects of the cancer problem, in: N. Weiner, J.P. Schade (Eds.), Progress in Cybernetics, Elsevier, Amsterdam, 1965.

[4] V.R. Potter, The role of nutrition in cancer prevention, Science 101 (1945) 105–109.

[5] J.E. Trosko, C.C. Chang, B.V. Madhukar, Modulation of intercellular communication during radiation and chemical carcinogenesis, Radiat. Res. 123 (1990) 241–51.

[6] E. Mamontov, A. Koptioug, K. Psiuk-Maksymowicz, The minimal, phase-transition model for the cell-number maintenance by the hyperplasia-extended homeorhesis, Acta Biotheor. 54 (2006) accepted.

[7] A.V. Koptioug, E. Mamontov, Toward prevention of hyperplasia in oncogeny and other proliferative diseases: the role of the cell genotoxicity in the model-based strategies, in: 7th Ann. Conf. in Göteborg, Sweden, "Functional Genomics – From Birth to Death", 19-20 August, 2004. Programme and Abstract Book, 1pp. abstract, oral presentation, and poster. Göteborg, Göteborg Univ.; http://funcgenomics.lundberg.gu.se/ (2004).

[8] A.V. Koptioug, E. Mamontov, Z. Taib, M. Willander, The phase-transition morphogenic model for oncogeny as a genotoxic dysfunction: interdependence of modeling, advanced measurements, and numerical simulation, in: ICSB2004, 5th Int. Conf. Systems Biology, 9-13 October, 2004, 1pp. abstract and poster. Heidelberg; http://www.icsb2004.org/ (2004).

[9] M.B. Spornand, A.B. Roberts, Introduction: autocrine, paracrine and endocrine mechanisms of growth control, Cancer Surv. 4 (1985) 627–632.

[10] S.Y. Shvartsman, H.S. Wiley, W.M. Deen, D.A. Lauffenburger, Spatial range of autocrine signaling: modeling and computational analysis, Biophys. J. 81 (2001) 1854–1867.

[11] C.H. Waddington, Towards a theoretical biology, Nature 218 (1968) 525–527.

[12] D. Sauvant, Systematic modelling in nutrition, Reprod. Nutr. Dev. 32 (1992) 217–230.

[13] E. Mamontov, K. Psiuk-Maksymowicz, A. Koptioug, Stochastic mechanics in the context of the properties of living systems, Math. Comput. Model. (2006) accepted.

[14] W.B. Cannon, The Wisdom of the Body, Norton, New York, 1932.

[15] Y.V. Mamontov, M. Willander, Asymptotic method of finite equation for bounded solutions of nonlinear smooth ODEs, Math. Japonica 46 (1997) 451–461.

[16] E. Mamontov, Nonstationary invariant distribution and the hydrodynamic-style generalization of the Kolmogorov-Forward/Fokker-Planck equation, Appl. Math. Lett. 18 (2005) 976–982.

[17] E. Haus, M.H. Smolensky, Biologic rhythms in the immune system, Chronobiol. Int. 16 (1999) 581–622.

[18] F. Schlögl, Chemical reaction models for non-equilibrium phase transitions, Z. Phys. 253 (1972) 147–161.

[19] B.G. Katzung, Basic and Clinical Pharmacology, Lange Medical Books/McGraw-Hill, NewYork, 2001.

[20] G.A. Ezzell, J.M. Galvin, D. Low, J.R. Palta, I. Rosen, P. Xia, Y. Xiao, L. Xing, C.X. Yu, Guidance document on delivery, treatment planning, and clinical implementation of IMRT: report of the IMRT Subcommittee of the AAPM Radiation Therapy Committee, Med. Phys. 30 (2003) 2089–2115.

[21] K. Psiuk-Maksymowicz, A phase-transition-based, nonlinear reaction-diffusion equation for hyperplastic tumours and an analytical-numerical computer simulation, in: Workshop on Angiogenesis and Other Aspects of Tumour Growth, 15 July, 2005. Oral presentation, Warsaw; http://www.mimuw.edu.pl/∼biolmat/program_june.html (2005).

[22] K. Psiuk-Maksymowicz, E. Mamontov, The time-slice method for fast analysis of oncogenic hyperplasia, in: European Conference on Mathematical and Theoretical Biology - ECMTB05 (July 18-22, 2005, Dresden). Book of Abstracts, Vol. 1 (Center for Information Services and High-Performance Computing, Dresden University of Technology, Dresdn, 2005), p. 429.

[23] J.S. Bedford, W.C. Dewey, Historical and current highlights in radiation biology: Has anything important been learned by irradiating cells?, Radiat. Res. 158 (2002) 251–291.

[24] A. DeWitt, J.Y. Dong, H.S. Wiley, D. Lauffenburger, Quantitative analysis of the TGF receptor autocrine system reveals cryptic regulation of the cell response by ligand capture, J. Cell Sci. 114 (2001) 2301–2313.

[25] M.A.J. Chaplain, L. Graziano, L. Preziosi, Mathematical modelling of the loss of tissue compression responsiveness and its role in solid tumour development, Math. Med. Biol. (2006) accepted.